

# Chemistry of photogenerated $\alpha$ -hydroxy-*p*-nitrobenzyl carbanions in aqueous solution: protonation vs. disproportionation

James Morrison, Peter Wan, John E.T. Corrie, and V. Ranjit N. Munasinghe

**Abstract:** The photochemistry of *p*-nitrobenzyl derivatives **6–10** has been studied in aqueous solution as a function of pH, using product analysis, UV–vis spectrophotometry, and laser flash photolysis (LFP). The compounds were chosen with the aim of further exploring the propensity of these systems to give rise to  $\alpha$ -hydroxy-*p*-nitrobenzyl carbanions on photolysis, and to study their mechanisms of subsequent reaction.  $\alpha$ -Hydroxy-substituted carbanions are anions that cannot be readily formed using thermal routes but which are believed to have some interesting chemistry. Three methods were employed for photogenerating these carbanions: (i) decarboxylation; (ii) retro-Aldol reaction; and (iii) carbon acid deprotonation. All three methods proved to be successful using the *p*-nitrobenzyl chromophore. Photogenerated  $\alpha$ -hydroxy-*p*-nitrobenzyl carbanions react via disproportionation, giving rise to oxidized and reduced products; simple protonation of the anion was undetectable.

**Key words:** photodecarboxylation, nitrobenzyl carbanions, photoredox, nitroaromatic compounds, excited-state carbon acids.

**Résumé :** Opérant en solutions aqueuses en fonction du pH et faisant appel à l'analyse des produits, à la spectrophotométrie UV–vis et à la photolyse éclair au laser, on a étudié la photochimie des dérivés *p*-nitrobenzyles (**6–10**). On a choisi les composés dans le but de pouvoir explorer plus à fond la propension de ces systèmes de donner naissance à des carbanions  $\alpha$ -hydroxy-*p*-nitrophényles par photolyse et d'étudier les mécanismes de leur réaction subséquente. Les carbanions portant un substituant  $\alpha$ -hydroxy sont des anions qui ne peuvent pas se former facilement par les voies thermiques, mais que l'on soupçonne d'avoir des propriétés chimiques intéressantes. On a utilisé trois méthodes pour la photogénération de ces carbanions: (i) la décarboxylation; (ii) la réaction rétroaldolique et (iii) la déprotonation d'un acide carbonique. Ces trois méthodes ont été couronnées de succès avec le chromophore *p*-nitrobenzyle. Les carbanions  $\alpha$ -hydroxy-*p*-nitrobenzyles photogénérés réagissent par une réaction de métathèse qui conduit à la formation de produits oxydés et de produits réduits; on n'a pas pu mettre en évidence de protonation simple de l'anion.

**Mots clés :** photodécarboxylation, carbanions nitrobenzyles, photorédox, composés nitroaromatiques, état excité d'acides carbonés.

[Traduit par la Rédaction]

## Introduction

Carbanions are synthetically useful and fundamentally important reactive intermediates in organic chemistry (1). The reactivity of carbanions as either nucleophiles, bases, or as electron donors is well-known and substituents strongly influence their stability and reactivity. This is exemplified by the enormous range of carbon acid  $pK_a$  values (1) and these data are useful in predicting the conditions necessary to generate a carbanion and its subsequent reactivity. Substituent effects on the negatively charged intermediate may be manifested through resonance, inductive effects, or by providing a new reaction pathway.  $\alpha$ -Hydroxy carbanions **1**, in which

an hydroxy group (an oxygen acid) is directly attached to the carbanion, are an interesting type of carbanion whose formation and stability has been the subject of theoretical interest (2, 3). However, for obvious reasons, the breadth of experimental knowledge of these carbanions is quite limited. Nonetheless,  $\alpha$ -hydroxy carbanions have been proposed as intermediates in photochemical (4–6) and enzymatically catalyzed (7, 8) reactions.



Received 3 January 2003. Published on the NRC Research Press Web site at <http://canjchem.nrc.ca> on 26 May 2003.

*Dedicated to Professor Don Arnold for his contributions to chemistry.*

**J. Morrison and P. Wan.**<sup>1</sup> Department of Chemistry, Box 3065, University of Victoria, Victoria, BC V8W 3V6, Canada.

**J.E.T. Corrie<sup>2</sup> and V.R.N. Munasinghe.** National Institute for Medical Research, The Ridgeway, Mill Hill, London, NW7 1AA, U.K.

<sup>1</sup>Corresponding author (e-mail: [pwan@uvic.ca](mailto:pwan@uvic.ca)).

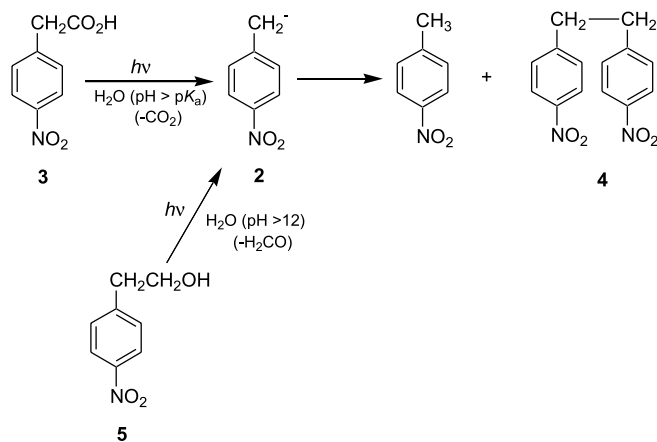
<sup>2</sup>Corresponding author (e-mail: [jcorrie@nimr.mrc.ac.uk](mailto:jcorrie@nimr.mrc.ac.uk)).

To study “free” carbanions in solution it is advantageous to generate appreciable amounts of these intermediates quickly. A well-known route is via photochemical reaction (9), preferably one that is fast and efficient. The simplest conceivable photochemical route to a carbanion is via a heterolytic C—C or C—H bond cleavage, for example via photodecarboxylation or photodeprotonation, respectively. Nitrobenzyl compounds, with their electron-withdrawing nitro group, are particularly adept at inducing these photocleavage reactions, generally via the triplet excited state (10, 11). While it is well-known that *o*-nitrobenzyl systems are highly photoreactive (generally via initial transfer of the benzylic hydrogen to the nitro group), the *m*- and *p*-isomers also display a range of photochemical reactivity not often reported for the *o*-isomer (10, 11). Both *m*- and *p*-nitrobenzyl compounds are known to undergo a variety of photofragmentation reactions, such as photodecarboxylation (12), photodeprotonation (4), and photoretro-aldol reaction (13), all of which have been proposed to generate *m*- and *p*-nitrobenzyl carbanions as intermediates. However, prior to our studies, only the parent *p*-nitrobenzyl carbanion was observed by transient methods (vide infra).

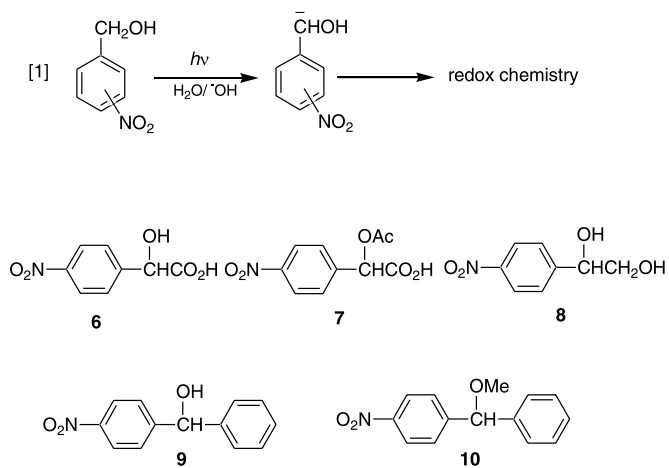
Margerum and Petrusis (12) were the first to investigate the chemistry of photogenerated *p*-nitrobenzyl carbanion (2), which they prepared by photodecarboxylation of *p*-nitrophenylacetic acid (3) (Scheme 1). The observed chemistry of photogenerated 2, to give *p*-nitrotoluene (simple protonation) and *p,p'*-dinitrobenzyl (4) (disproportionation product), may be described as “conventional” *p*-nitrobenzyl carbanion chemistry since thermally generated 2 (formed by deprotonation of *p*-nitrotoluene in *tert*-butyl alcohol – KOH) has also been observed to give 4 (14–16). Carbanion 2 is strongly stabilized by the *p*-nitrophenyl ring and is thus readily observable by UV–vis spectrophotometry as well as by  $\mu$ s and faster laser flash photolysis (LFP) ( $\lambda_{\max}$  358 nm;  $\tau$  = 53 s at pH 13) (12). The complex decay kinetics of carbanion 2 (mixed first- and second-order) were studied in some detail by Craig et al. (17, 18), who explained the data as arising via two competing pathways of reaction: (i) a simple protonation pathway to give *p*-nitrotoluene; and (ii) a bimolecular coupling pathway (of two molecules of 2), followed by loss of two electrons (the final fate of which was not determined) to form 4. Wan and Muralidharan (13) discovered a second method for generating carbanion 2, by base-catalyzed photoretro-aldol reaction of 5, with subsequent chemistry identical to that reported above.

The chemistry of  $\alpha$ -hydroxy-nitrobenzyl carbanions is not as well understood. Wan and Yates (4) first proposed water and hydroxide-mediated photodeprotonation of the benzylic proton of *m*- and *p*-nitrobenzyl alcohols, to give the corresponding  $\alpha$ -hydroxy nitrobenzyl carbanions (eq. [1]). In retrospect, the proposal of C—H bond deprotonation in the excited (triplet) state as a primary step was unusual, as there was no precedent for such a pathway at the time. In addition, reprotonation of these carbanions apparently does not occur, as shown by the absence of deuterium exchange, but instead redox chemistry was observed (4). *p*-Nitrobenzyl alcohol was found to give a simple intramolecular redox product in base (*p*-nitrosobenzaldehyde), whereas *m*-nitrobenzyl alcohol gave a mixture of *m*-nitrobenzaldehyde (60–70%) and *m*-azoxybenzaldehyde (40–30%) (in neutral, acid, and basic

Scheme 1.

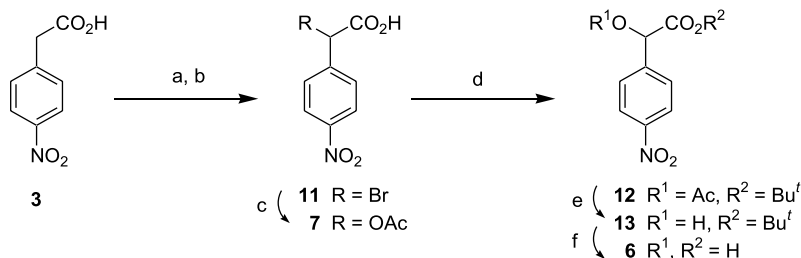


solutions), via an apparent disproportionation of the photogenerated carbanion. Disproportionation chemistry has also been observed for photogenerated  $\alpha$ -hydroxy-*p*-(*p*-nitrophenyl)benzyl carbanion in neutral solution (6). The observation of disproportionation and redox pathways is perhaps not unexpected considering that even the parent *p*-nitrobenzyl carbanion (2) displays this kind of reactivity. Moreover, theoretical calculations (3) have shown that simple anions (in the gas phase) such as  $\text{CH}_2\text{OH}^-$  and  $\text{CH}_2\text{NH}_2^-$  are unstable with respect to their radicals. This suggests that carbanions of this kind have an intrinsic propensity for disproportionation chemistry (for example, via initial electron transfer). Some of the products described above (4, 6) are consistent with this pathway.



The aim of this work is to study in more detail the chemistry of a variety of photogenerated  $\alpha$ -hydroxy-*p*-nitrobenzyl carbanions (1,  $R' = p$ -nitrophenyl) and related species, using product studies and LFP. For this purpose *p*-nitromandelic acid (6) and its *O*-acetyl derivative 7 are obvious initial substrates since it is anticipated that these compounds will undergo efficient photodecarboxylation, to give the corresponding  $\alpha$ -hydroxy and  $\alpha$ -acetoxy-*p*-nitrobenzyl carbanions. *p*-Nitrophenylethylene glycol (8) would be expected to undergo base-catalyzed photoretro-aldol reaction to give the parent  $\alpha$ -hydroxy-*p*-nitrobenzyl carbanion in basic medium. Finally, *p*-nitrobenzyl alcohol (9), and the corresponding methyl

**Scheme 2.** Synthesis of **6** and **7**. Reagents and conditions: (a)  $\text{SOCl}_2$ ; (b)  $\text{Br}_2$ ; (c)  $\text{Hg}(\text{OAc})_2$ ,  $\text{HOAc}$ ; (d)  $\text{Cl}_3\text{C}(\text{NH})\text{O}-t\text{-Bu}$ ,  $\text{CH}_2\text{Cl}_2$ ; (e)  $\text{CsCO}_3$ ,  $\text{MeOH}$ ; (f)  $\text{TFA}$ .



ether **10** are expected to give  $\alpha$ -hydroxy (or methoxy) *p*-nitrobenzyl carbanions via photodeprotonation.

## Results and discussion

### Materials

*p*-Nitromandelic acid (**6**) is only sporadically reported in the literature and its synthesis, unlike that of the corresponding *o*-nitro isomer (**19**), is surprisingly difficult. In our hands the complex procedure described by Carrara et al. (20), based on formation of *p*-nitromandelonitrile and subsequent acidic hydrolysis, was not reproducible. We, therefore, adopted the route shown in Scheme 2 which yielded first the *O*-acetyl derivative **7**. Because of concerns about the stability of **6** under basic conditions and possible difficulties of isolation, we chose to prepare it via the *tert*-butyl ester **12**. Subsequent mild base treatment ( $\text{CsCO}_3$  in methanol) gave the alcohol **13**, from which **6** was obtained by TFA-mediated cleavage of the *tert*-butyl group.

Glycol **8** was available from a previous study (21). *p*-Nitrobenzhydrol (**9**) and its methyl ether derivative **10** were made by standard methods (see *Experimental*).

### Product studies

UV-vis spectrophotometry was used as a quick and informative tool to monitor the photochemistry of substrates **6–10** under various conditions and preparative photolyses were used to identify products formed. Photolysis of *p*-nitromandelic acid (**6**) as its carboxylate salt (~100%  $\text{H}_2\text{O}$ , pH 7, Ar purged, Rayonet photoreactor, 300 nm) in a UV cuvette resulted in formation of new (permanent) absorption bands at 289 and 308 nm (Fig. 1). No transient species was observed on this time scale. Strikingly different spectral changes that imply different photochemistry were observed upon photolysis of the *O*-acetyl derivative **7** (Fig. 2). A strong absorption band at 369 nm that was observed immediately after brief irradiation (Ar purged) decayed via complex kinetics over the course of several minutes (Fig. 3; the decay cannot be satisfactorily fitted to either first- or second-order kinetics; it is assumed to be a mixture of these components). The overall decay was slower in  $\text{D}_2\text{O}$ , consistent with a component of the processes involving proton (deuteron) transfer from solvent. The 369 nm absorption band was not observed using this technique upon photolysis of **7** in oxygen-saturated solution ( $\tau < 10$  s). These observations are very similar to those reported for the 358 nm absorption band of the parent *p*-nitrobenzyl carbanion (**2**) (**12**, **17**, **18**).

Therefore, the 369 nm transient is assigned to  $\alpha$ -acetoxy-*p*-nitrobenzyl carbanion (**14**).

Preparative photolysis of **6** and **7** ( $1 \times 10^{-3}$  M, 1:1  $\text{H}_2\text{O}-\text{CH}_3\text{CN}$ , Rayonet photoreactor, 300 nm) confirmed the observations from UV-vis spectrophotometry that indicated different reaction pathways for these compounds. Low conversion runs (<30%) of **6** at pH 7 (Ar purged) followed by product isolation gave *p*-nitrobenzaldehyde (**15**) and *p,p'*-azoxybisbenzaldehyde (**16**) (Scheme 3). The relative yields of **15** and **16** (60–70% and 40–30%, respectively) were independent of conversion (up to ~40%), consistent with both being primary photoproducts. These are the expected disproportionation products of an  $\alpha$ -hydroxy-*p*-nitrobenzyl carbanion intermediate, analogous to the reported products of the photochemistry of *m*-nitrobenzyl alcohol (**4**) and *p*-(*p*-nitrophenyl)benzyl alcohol (**6**). At high conversion (>50%) insoluble orange precipitates and some soluble (but unidentified) secondary photoproducts were observed. Photolysis of **6** in oxygen-saturated solution gave mostly **15** (>90%) and some minor unidentified products. At pH 13 (Ar purged), low conversion (~15%) runs gave **15** and **16** (60–70% and 40–30%, respectively, as at pH 7). Photolysis at pH 3 gave the intramolecular redox product *p*-nitrosobenzaldehyde (**17**) in addition to **15** and **16** (relative yields 28:50:22). The formation of **17** in acidic solution is reminiscent of the intramolecular photoredox chemistry reported for *p*-nitrobiphenyl systems (**6**). We were not able to enhance the relative yield of **17** since the photodecarboxylation quantum yield becomes negligible in solutions below pH 3, because ionization of the carboxylic acid is suppressed. For example, irradiation of **6** at pH 1 resulted in quantitative recovery of substrate. These observations are consistent with a mechanism in which **17** must arise via initial decarboxylation of the ionized form of **6**. The requirement of an acidic solution for formation of **17** will be discussed later.

Preparative photolysis of **7** (pH 7, Ar purged) gave the product of simple decarboxylation, i.e., *p*-nitrobenzyl acetate (**18**) and the expected disproportionation product,  $\alpha,\alpha'$ -bisacetoxy-*p,p'*-dinitrobenzyl (**19**) (eq. [2]). The relative yield of **18** to **19** was ~ 1:1 in  $\text{H}_2\text{O}-\text{CH}_3\text{CN}$  but this ratio was dramatically altered in 1:1  $\text{D}_2\text{O}-\text{CH}_3\text{CN}$  (~5%  $\alpha$ -deuterated **18** and ~95% **19**). Thus, when the protonation pathway (**14**  $\rightarrow$  **18**) is retarded in  $\text{D}_2\text{O}$  by a primary solvent isotope effect, the disproportionation pathway that gives **19** becomes dominant. Photolysis of **7** in oxygen-saturated solution gave **15** (60%) and *p*-nitrobenzoic acid (40%); neither **18** nor **19** was observed. This indicates that interception of

**Fig. 1.** UV-vis traces observed on photolysis of **6** in ~100% H<sub>2</sub>O ( $6.6 \times 10^{-5}$  M, 0.01 M pH 7 phosphate buffer, Ar purged). Each trace represents 15 s irradiation at 300 nm (4 lamps). Arrows indicate changes in absorbance.

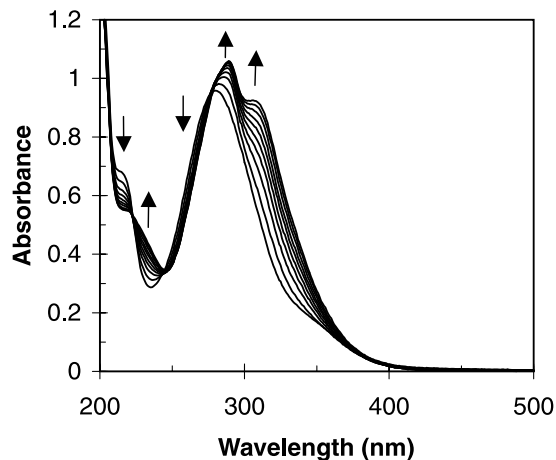
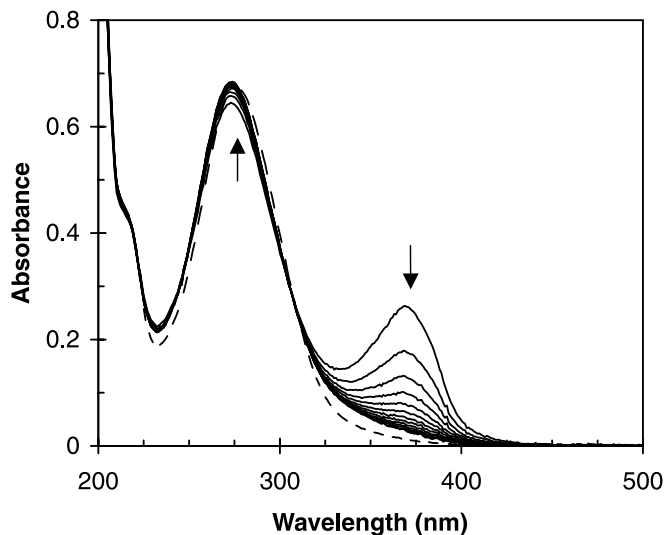
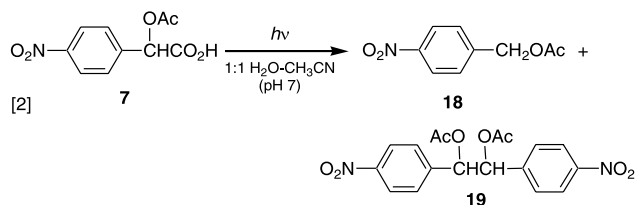


**Fig. 2.** UV-vis traces observed before (dashed line) and immediately following 15 s photolysis (300 nm, 16 lamps) of **7** in ~100% H<sub>2</sub>O (solid lines) ( $6.7 \times 10^{-5}$  M, 0.01 M pH 7 phosphate buffer, Ar purged). Each trace of the dark reaction is separated by 30 s. Arrows indicate changes in absorbance during the dark reaction.

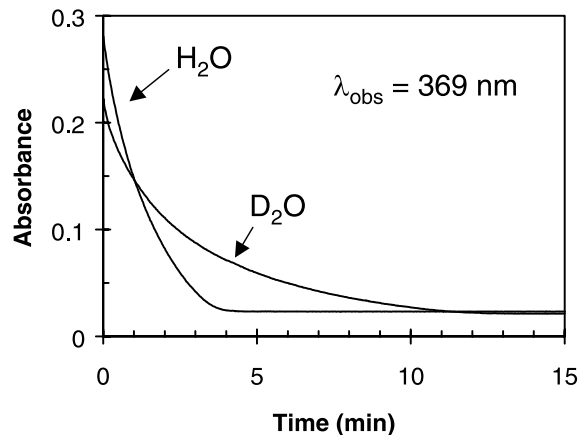


**14** by dissolved oxygen is much more efficient than either protonation or disproportionation.

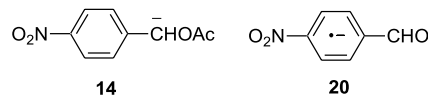


*p*-Nitrophenylethylene glycol (**8**) was found to be photo-reactive only in basic solution. UV-vis traces of the reaction (~100% H<sub>2</sub>O, pH 13, Ar purged) allowed observation of a

**Fig. 3.** Decay in absorbance of **14** photogenerated from **7** in ~100% H<sub>2</sub>O (complete within 5 min) or ~100% D<sub>2</sub>O (complete within 15 min) measured at 369 nm immediately following 15 s photolysis ( $6.7 \times 10^{-5}$  M, 300 nm, 16 lamps, pH(D) 7, Ar purged). Neither trace could be fitted satisfactorily to a first- or second-order kinetic equation.



strong transient absorption band at  $\lambda_{\max}$  403 nm that decayed within 1 h (Fig. 4) with complex kinetics (Fig. 4, inset). The initial decay appears to obey first-order kinetics; however, after approximately 20 min the decay becomes (reproducibly) more complex, suggestive of contributions from competing reactions. This transient was observed only in basic solution (Fig. 5); no spectral changes were observed in neutral or acidic solution (below pH 11), even on prolonged irradiation. The transient was also not observed in oxygen-saturated basic solution.



Preparative photolysis of **8** ( $1 \times 10^{-3}$  M, pH 13, Ar) gave **15** and **16** (60–70% and 40–30%, respectively), as observed for **6** in neutral or basic solution. In keeping with the cuvette results above, no reaction was observed at pH 7. Base catalysis of the reaction of **8** is in line with observations made for **5** (13), although the latter is not known to give an observable 403 nm transient. In a previous study of **8** in our laboratory (21), a long-lived radical anion species was photogenerated and assigned from its ESR spectrum as *p*-nitrobenzaldehyde radical anion (**20**). Its lifetime in the ESR spectrum was similar to that observed for the transient 403 nm absorption band. Radical anion **20** has previously been reported to have an absorption maximum of ~400 nm (22) and the present data are in good agreement with this.

Irradiation of *p*-nitrobenzhydrol (**9**) at pH 13 (~100% H<sub>2</sub>O, Ar purged, 300 nm) in a UV cuvette resulted in initial spectral changes that were consistent with formation of **21**. However, other components were evidently present, as the initial spectrum was not stable over time and underwent complex changes over the course of 10–30 min in the absence of light, indicating that relatively slow dark processes were occurring. No spectral changes were observed at pH 7, consistent with base catalysis of photoreaction. Preparative

## Scheme 3.

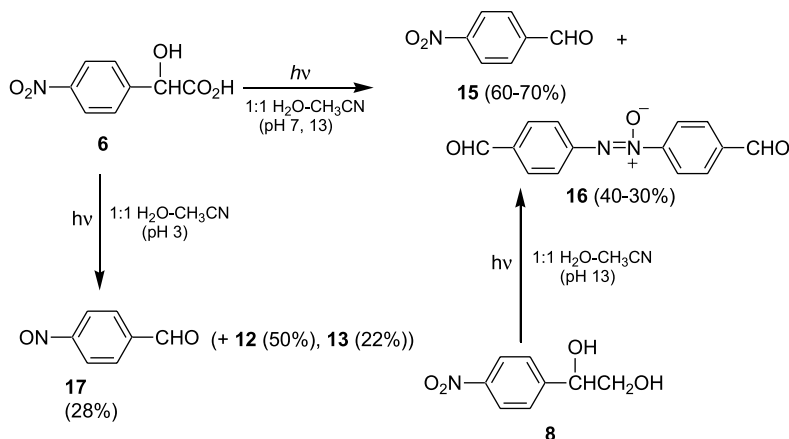
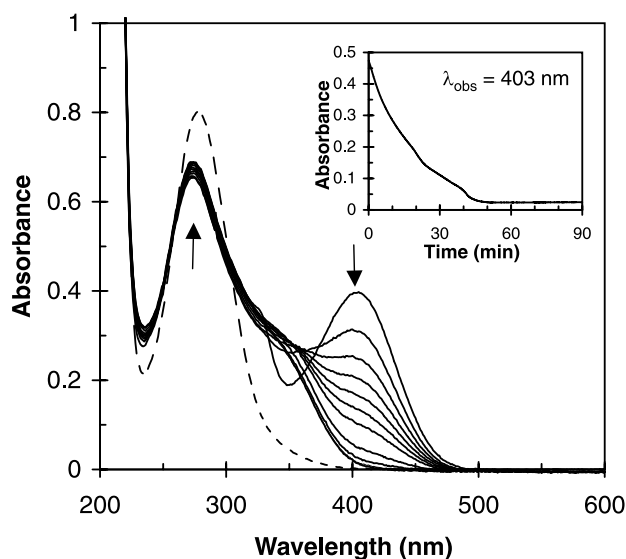
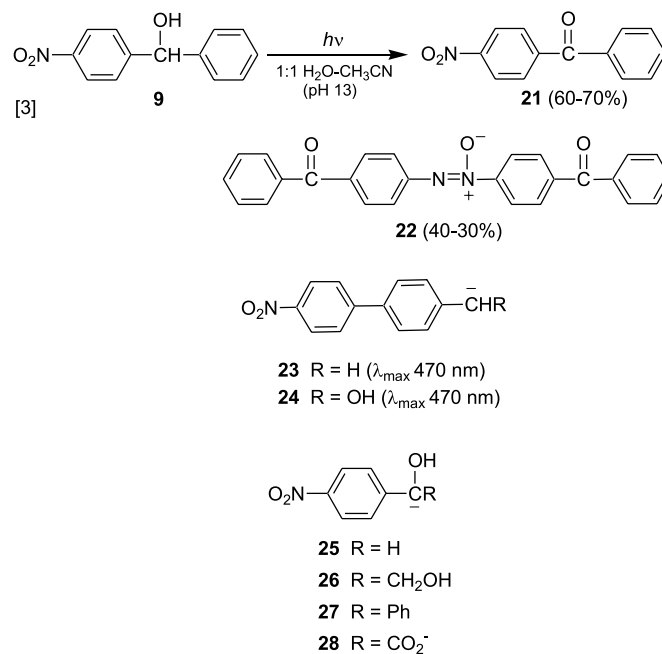


**Fig. 4.** UV-vis traces observed before (dashed line) and immediately following 30 s photolysis (300 nm, 16 lamps) of **8** in ~100% pH 13 H<sub>2</sub>O ( $7.4 \times 10^{-5}$  M, Ar purged). Each trace is separated by 5 min (solid lines). Arrows indicate changes in absorbance during the dark reaction. Inset: observed decay of the 403 nm absorption band.



photolysis of **9** ( $1 \times 10^{-3}$  M, 1:1 H<sub>2</sub>O-CH<sub>3</sub>CN, pH 13) gave two isolable disproportionation products, *p*-nitrobenzophenone (**21**) and *p,p'*-azoxybisbenzophenone (**22**) (60–70 and 40–30% relative yield, respectively), and a third minor (<10%, relative to **21**) product that has not been fully characterized but is believed to be derived from further reduction of **22** (see *Experimental*) (eq. [3]). Observation of base-catalyzed products from **9**, which is reminiscent of the photochemistry of *m*- and *p*-nitrobenzyl alcohol (**4**), suggests that the reaction pathway involves initial deprotonation from the benzylic position of **9**. However, attempts to trap the  $\alpha$ -hydroxybenzyl carbanion intermediate from **9** with D<sub>2</sub>O (at pD 13) were unsuccessful. Thus, extended photolysis of **9** in 1:1 D<sub>2</sub>O-CH<sub>3</sub>CN (pD 13) to >80% conversion followed by recovery of unreacted substrate showed complete absence of deuterium incorporation at the methine position (as monitored by <sup>1</sup>H NMR integration of this signal relative to the ar-

omatic signals). This is in agreement with previous studies of *m*- and *p*-nitrobenzyl alcohols (**4**), in which the corresponding photogenerated carbanions were also found not to undergo deuterium incorporation at the benzylic position. *p*-Nitrobenzhydryl methyl ether (**10**) might be expected to display “conventional” *p*-nitrobenzyl carbanion chemistry upon photodeprotonation, which would lead to deuterium incorporation. However, prolonged irradiation of **10** (pD 13, 10 h) resulted in complete recovery of substrate, with no evidence of deuterium exchange.



The quantum yield for reaction of **6** was estimated using *p*-nitrophenylacetic acid (**3**) ( $\Phi = 0.6$ ) (**12**, **17**) as secondary actinometer. Comparative photolysis of **3** and **6** to low conversion (<20%) gave a quantum yield for the reaction of **6** in 100% H<sub>2</sub>O (pH 6) of  $0.4 \pm 0.1$ . Quantum yields for reaction of **7** (pH 7), **8** (pH 14), and **9** (pH 13) were also estimated using product analysis and were 0.4, 0.5, and 0.02, respectively.

**Fig. 5.** Initial change in 403 nm absorbance ( $\Delta OD = OD$  immediately after irradiation minus  $OD$  before irradiation) upon irradiation of **8** in  $\sim 100\%$  H<sub>2</sub>O, pH 1–14 (300 nm, 16 lamps, 15 s photolysis time,  $7.4 \times 10^{-5}$  M, Ar purged).

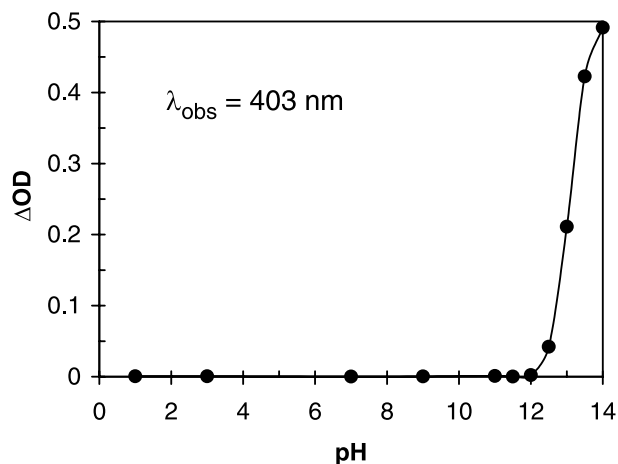
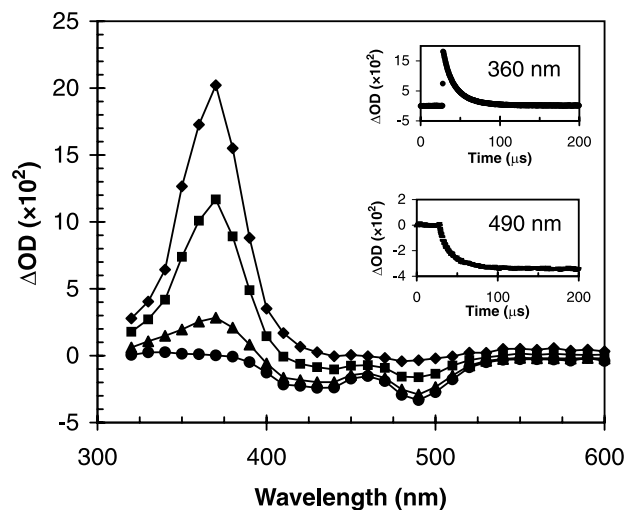


**Fig. 6.** LFP traces for **7** ( $4.7 \times 10^{-5}$  M) with  $1 \times 10^{-4}$  M IrCl<sub>6</sub><sup>2-</sup> in  $\sim 100\%$  H<sub>2</sub>O (pH 7, N<sub>2</sub> purged,  $\lambda_{ex}$  308 nm). Diamonds represent the spectrum sampled 1.8  $\mu$ s after the laser pulse, which includes carbanion **14** at 369 nm. Squares and triangles (sampled at 9.2 and 34  $\mu$ s) represent the decay of the 369 nm band simultaneous with the bleaching of the IrCl<sub>6</sub><sup>2-</sup> absorption bands at 430 and 490 nm to the final spectrum (at 130  $\mu$ s) represented by circles. Top inset: decay of carbanion **14** ( $k_{obs} = 6.2 \times 10^4$  s<sup>-1</sup>, monitored at 360 nm). Bottom inset: bleaching of IrCl<sub>6</sub><sup>2-</sup> ( $k_{obs} = 6.2 \times 10^4$  s<sup>-1</sup>, monitored at 490 nm).



### Laser flash photolysis

*p*-Nitrobenzyl carbanion **2** (which absorbs strongly at  $\lambda_{max}$  358 nm) has been extensively studied by transient methods (12, 17). Its lifetime is sensitive to pH but not to oxygen and is shortened in the presence of IrCl<sub>6</sub><sup>2-</sup> that acts as a one-electron acceptor (23–25). When the  $\pi$  system is further extended with another phenyl ring, as is the case for *p*-(*p*'-nitrophenyl)benzyl carbanion (**23**), the absorption maximum is at much longer wavelength ( $\lambda_{max}$  470 nm) (6). Further

**Fig. 7.** LFP traces for **6** in  $\sim 100\%$  H<sub>2</sub>O, pH 6.0 ( $4.6 \times 10^{-5}$  M, 0.01 M phosphate buffer, N<sub>2</sub> purged,  $\lambda_{ex}$  266 nm). Diamonds represent the spectrum sampled 700 ns after the laser pulse, which includes  $\alpha$ -hydroxy carbanion **25** at 360 nm. Squares and triangles represent the decay of the spectrum at 2.6 and 6.9  $\mu$ s after the laser pulse, respectively. Final spectrum after the decay (sampled at 36  $\mu$ s) of **25** to the product at 340 nm is represented by circles. Top inset: decay of carbanion **25** ( $k_{obs} = 2.6 \times 10^5$  s<sup>-1</sup>, monitored at 360 nm). Bottom inset: growth of product ( $k_{obs} = 3.1 \times 10^5$  s<sup>-1</sup>, monitored at 290 nm).

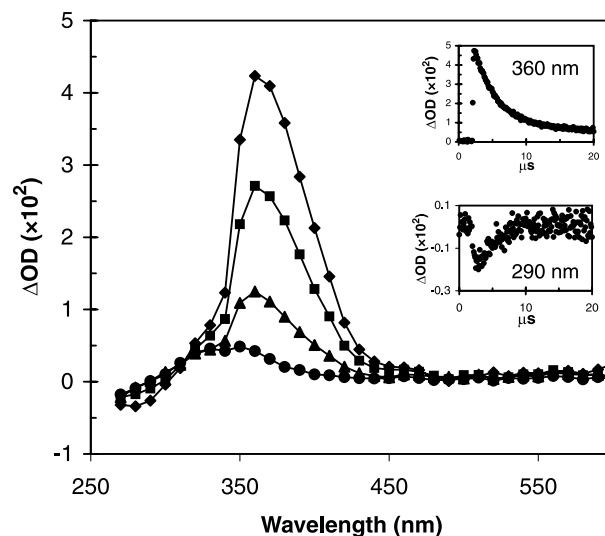
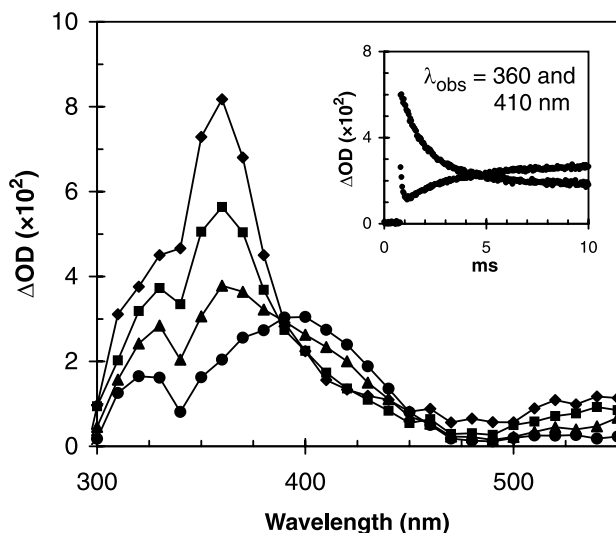


**Fig. 8.** LFP traces for **8** in  $\sim 100\%$  H<sub>2</sub>O, pH 13.0 ( $5.7 \times 10^{-5}$  M, N<sub>2</sub> purged,  $\lambda_{ex}$  266 nm) which includes  $\alpha$ -hydroxy carbanion **25** at 360 nm. Squares and triangles represent decay of the spectrum at 900  $\mu$ s and 2.8 ms, respectively. After the decay of **25** was complete, the spectrum of radical anion **20** was observed; represented by circles, sampled at 14 ms after the laser pulse. Inset: Decay of **25** ( $k_{obs} = 6.7 \times 10^{-2}$  s<sup>-1</sup>, monitored at 360 nm) is simultaneous with the growth of radical anion **20** ( $k_{obs} = 4.2 \times 10^{-2}$  s<sup>-1</sup>, monitored at 410 nm).



substitution of the carbanion with an  $\alpha$ -hydroxy group does not shift the absorption maximum, as  $\alpha$ -hydroxy-*p*-(*p*'-nitro-

**Fig. 9.** LFP traces observed for **9** in ~100% H<sub>2</sub>O, pH 13.0 ( $5.3 \times 10^{-5}$  M, N<sub>2</sub> purged,  $\lambda_{\text{ex}}$  266 nm). Diamonds represent the spectrum sampled 1.7  $\mu\text{s}$  after the laser pulse, which includes carbanion **27** at 460 nm. Squares and triangles represent decay of the spectrum, sampled at 8.6 and 28  $\mu\text{s}$ , respectively. Circles represent spectrum after the decay of **27** at 77  $\mu\text{s}$ . Inset: decay of **27** ( $k_{\text{obs}} = 5.2 \times 10^4 \text{ s}^{-1}$ , observed at 460 nm).

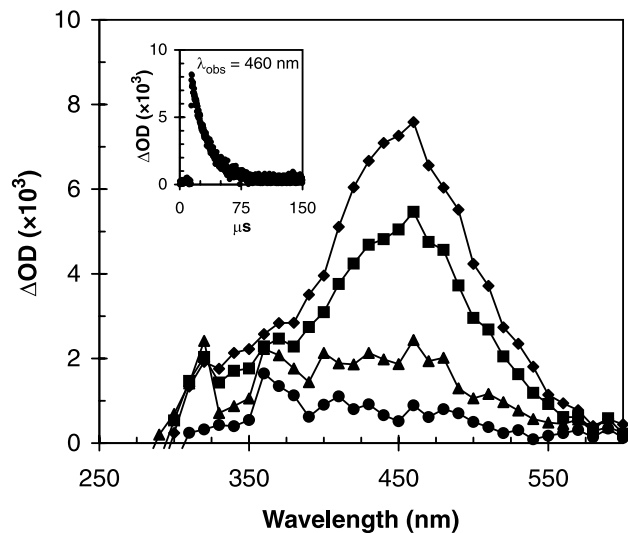
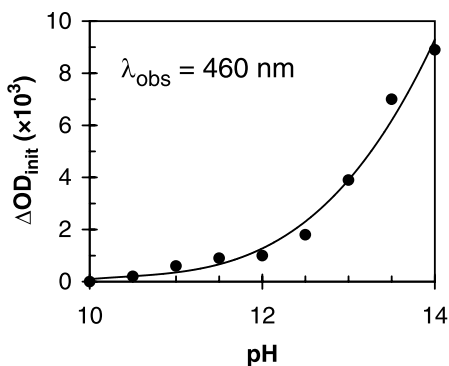


**Fig. 10.** Plot of the initial change in absorbance ( $\Delta\text{OD}_{\text{init}}$ ) at 460 nm upon LFP of **9** at pH 10–14 ( $5.3 \times 10^{-5}$  M, ~100% H<sub>2</sub>O, N<sub>2</sub> purged,  $\lambda_{\text{ex}}$  266 nm). Each point represents the average initial  $\Delta\text{OD}$  observed for 10 shots, assigned to carbanion **27** formed by photodeprotonation of **9**.



phenyl)benzyl carbanion (**24**) was also observed at 470 nm (**6**). Thus, it was anticipated that the *p*-nitrobenzyl carbanions generated from **6–8** should also have absorption maxima near 360 nm. This indeed was found to be the case for carbanion **14** formed from **7** ( $\lambda_{\text{max}}$  369 nm, vide supra), which was sufficiently long-lived to allow detection by conventional UV–vis spectrophotometry. LFP of **7** (266 nm, pH 7, ~100% H<sub>2</sub>O, N<sub>2</sub> purged) also gave **14** ( $\lambda_{\text{max}}$  369 nm) which did not decay within the 150 ms (longest possible) time window of our LFP system, consistent with it being a very long-lived species (vide supra). However, LFP of **7** in the presence of IrCl<sub>6</sub><sup>2-</sup> (308 nm, N<sub>2</sub> purged) showed an accelerated decay of the 369 nm transient that was simultaneous with bleaching of IrCl<sub>6</sub><sup>2-</sup> bands at 430 and 490 nm (Fig. 6).

**Fig. 11.** LFP traces observed for **6** in ~100% H<sub>2</sub>O, pH 13.0 ( $4.6 \times 10^{-5}$  M, N<sub>2</sub> purged,  $\lambda_{\text{ex}}$  266 nm). Diamonds represent the spectrum sampled 5.1  $\mu\text{s}$  after the laser pulse, which includes carbanion **28** (420 nm) formed by photodeprotonation of **6**, and carbanion **25** (360 nm) formed by photodecarboxylation of **6**. Squares and triangles represent partial decay of the spectrum (decay of **28** and not **25**), sampled at 26 and 69  $\mu\text{s}$ , respectively. Circles represent the spectrum after **28** has completely decayed, leaving **25** and possible products from **28**. Top inset: decay of **28** ( $k_{\text{obs}} = 2.1 \times 10^4 \text{ s}^{-1}$ , monitored at 420 nm). Bottom inset: growth of product from **28** ( $k_{\text{obs}} = 2.2 \times 10^4 \text{ s}^{-1}$ , monitored at 350 nm).

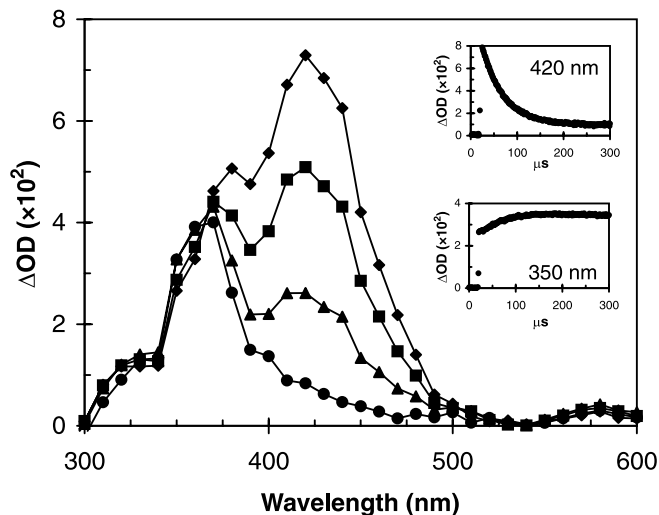
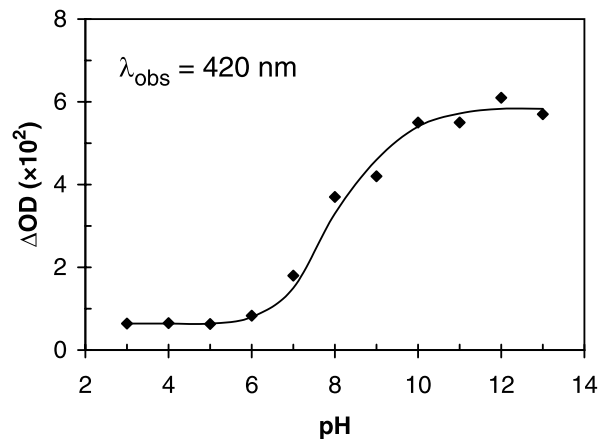


**Fig. 12.** Plot of the initial change in absorbance ( $\Delta\text{OD}_{\text{init}}$ ) at 420 nm upon LFP of **6** at pH 3–13 ( $4.6 \times 10^{-5}$  M, ~100% H<sub>2</sub>O, N<sub>2</sub> purged,  $\lambda_{\text{ex}}$  266 nm). Each point represents the average initial  $\Delta\text{OD}$  observed for 10 shots. Above pH 7  $\Delta\text{OD}_{\text{init}}$  is mostly attributed to carbanion **28** formed by direct carbon acid deprotonation. At pH 7 and below  $\Delta\text{OD}_{\text{init}}$  is mostly attributed to **25** formed by photodecarboxylation which has weak absorption at 420 nm (assignment based on lifetimes).



LFP of **6** (266 nm) at pH 6 gave a transient at ~360 nm with a similar absorption profile as that of carbanion **14** (Fig. 7). It decayed via first-order kinetics ( $\tau = 3.8 \mu\text{s}$ , 0.01 M phosphate buffer, pH 6) to a weaker but permanent absorption in the range 300–340 nm, assignable as a mixture

of **15** and **16**. Assignment of the 360 nm transient to **25** is based on its similarity to **14**. Additionally, LFP of **6** in the presence of  $\text{IrCl}_6^{2-}$  showed an accelerated decay of the 360 nm band in synchrony with bleaching of the  $\text{IrCl}_6^{2-}$  bands at 430 and 490 nm.

LFP of **8** at pH 13 also gave carbanion **25** ( $\tau = 1.5$  ms) as a transient (Fig. 8). No transients were observed at pH 7 consistent with its lack of photochemical reactivity in neutral solution (vide supra). Decay of **25** (at pH 13) was concomitant with the growth of a band at 400 nm, which did not decay within 150 ms (Fig. 8, inset). The long-lived 400 nm transient (not observed in the presence of oxygen) is assigned to radical anion **20**, which was also observed by UV-vis spectrophotometry (Fig. 4). Closer examination of the kinetic trace at 410 nm (Fig. 8, inset) also showed evidence of a shorter-lived species ( $\tau = 63$   $\mu\text{s}$ ) absorbing in this region, the identity of which is not known with certainty but which we have tentatively assigned to carbanion **26**, arising via benzylic deprotonation of **8**.

LFP of **9** at pH 13 gave a broad absorption band at 460 nm (Fig. 9) that decayed by first-order kinetics to baseline (Fig. 9, inset). The intensity of the 460 nm absorption was strongest at pH 14 and was progressively weaker at lower pH values; at pH 10 no signal was observable (Fig. 10). This apparent base catalysis of transient formation supports its assignment as carbanion **27**. Its absorption maximum is red-shifted by 100 nm compared to carbanion **25** ( $\lambda_{\text{ex}}$  360 nm) which is compatible with the extended conjugation available from the additional phenyl ring.

The LFP spectrum of **6** at pH 13 was dominated by a band at 420 nm (Fig. 11), which decayed ( $\tau = 47$   $\mu\text{s}$ ) to a long-lived ( $\tau > 150$  ms) 360 nm band. The  $\Delta\text{OD}$  of the 420 nm band as a function of pH is shown in Fig. 12, which has an apparent titration plot, suggesting that the 420 nm transient is carbanion **28** (with an excited state  $\text{pK}_a$  of  $\sim 8$  for the benzylic proton of **6**). This seems reasonable considering the analogous photodeprotonation observed for **9** at high pH.

### Mechanisms of reaction

Our study of the photochemistry of *p*-nitrobenzyl derivatives **6–10**, by a combination of product studies, UV-vis spectrophotometry, and LFP, has provided additional insights into their mechanisms of reaction. It seems clear that the aqueous photochemistry for all of **6–9** involves *p*-nitrobenzyl carbanions. Indeed, several  $\alpha$ -hydroxy-*p*-nitrobenzyl carbanions, generated by C—H bond deprotonation or by decarboxylation (or deformylation), were observed for the first time. With the present data, an overall mechanistic picture of the photochemistry of these compounds is now available.

Photodecarboxylation of **6** (assumed to be via  $T_1$ ) occurs with appreciable quantum efficiency at pH 3–13 to generate **25** (Scheme 4). The lack of photoreactivity of **6** and absence of an LFP signal attributable to **25** at pH values 1 and 2 indicate that photodecarboxylation only occurs via the carboxylate form of **6**. The necessary steps to generate products **15** and **16** from **25** most likely involve overall loss of an electron and a proton (sequentially or via one-step loss of a hydrogen atom), to generate radical anion **20** ( $\lambda_{\text{max}}$  403 nm, vide supra), which is known to be long-lived at high pH but undetectable at lower pH (21). Radical ion **20** has been

shown to lead to reduction product **16** (21), while scavenging of the electron of **20** by residual oxygen or on work-up would lead to **15**. The formation of **17** at pH 3 suggests an alternate pathway involving an overall intramolecular redox reaction for **25**. This new pathway is observed at a pH that coincides with significant protonation of the nitro group of **25**, to give **29** (similar *aci*-nitrobenzyl compounds have  $\text{pK}_a \sim 3$ , (6, 17, 26)). Net dehydration of **29** gives **17**.

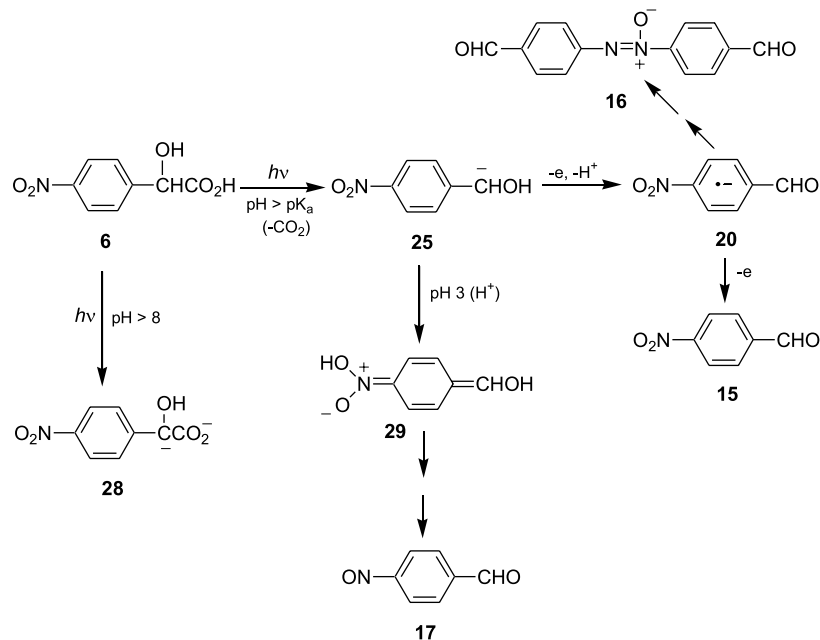
At pH values  $> 8$ , photoionization of the benzylic proton of **6** (to give **28**) apparently competes with photodecarboxylation, as shown in LFP studies, although to what extent is not entirely clear with the data available. We have not isolated any product at high pH that might be expected to arise via **28**, but only compounds **15** and **16** as seen at pH values in the range  $\sim 4$ – $7$ . The possibility of facile reprotonation of **28** to give back **6** (in the ground-state reaction) is a distinct possibility. However, we have not attempted any deuterium incorporation experiments at these high pHs because of the obvious complication of thermal background exchange in basic  $\text{D}_2\text{O}$ . Thus, further understanding of the competing benzylic C—H deprotonation of **6** requires additional studies.

The proposed reaction pathway for **8** (pH  $> 12$ ) (Scheme 5) is simpler. LFP observations at pH 13 indicate that generation of **25** from **8** occurs much more cleanly, with no significant photoionization at the benzylic position. Carbanion **25** (from **8**) gives radical anion **20** (via overall loss of an electron and a proton), as shown by growth of the radical anion absorption band ( $\lambda_{\text{max}}$  403 nm) concomitantly with decay of the absorption band of **25** ( $\lambda_{\text{max}}$  360 nm) (Fig. 8). The subsequent decay of **20** appears to be more complex, after a phase with initial first-order kinetics (Fig. 4, inset), and is suggestive of multistep pathways for subsequent formation of **16**.

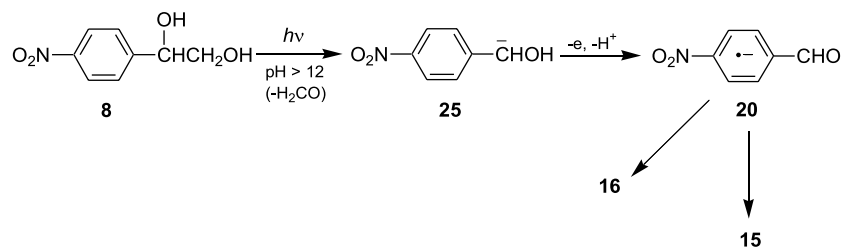
The  $\alpha$ -acetoxy carbanion **14** generated via photodecarboxylation of **7** behaves as a conventional *p*-nitrobenzyl carbanion (mimicking **2**, Scheme 1). The two observed products, **18** and **19**, arise via protonation and coupling pathways (giving a dianion, which subsequently loses two electrons to give **19**) (18). Given that the observed lifetime of **14** is very long compared to that of **25**, both its protonation and coupling processes must be slow. In contrast, the lifetime of **25** at pH 6 is more than 7 orders of magnitude shorter ( $\mu\text{s}$  vs. min). Clearly the disproportionation pathway available to **25** is sufficiently fast that protonation or coupling cannot compete. Comparison of the pseudo-first-order rate constants for reaction of these carbanions with  $\text{IrCl}_6^{2-}$  (**25** reacts only about 2 times faster than **14**) suggests that the oxidation potentials of **14** and **25** are roughly equivalent. Thus, the key structural feature that allows the efficient disproportionation pathway observed for **25** is the  $\alpha$ -hydroxyl proton. This is consistent with gas-phase theoretical calculations (3) that have shown anions such as  $^-\text{CH}_2\text{OH}$  and  $^-\text{CH}_2\text{NH}_2$  to be unstable with respect to their radicals.

The reaction pathway of **9** is similar in essence to those of **6** and **8**. It differs in that the carbanion **27** is formed by direct C—H bond heterolysis, and is the only *p*-nitrobenzyl carbanion that could form in this case. To our knowledge, only one other example of LFP observation of a carbanion generated by photoionization has been reported (6). The subsequent product-forming steps from **27** are believed to be similar to those proposed for **6** and **8**; i.e., the carbanion for-

Scheme 4.



Scheme 5.



mally loses a hydrogen atom to form the corresponding radical anion, which subsequently disproportionates to products **21** and **22**. The complete absence of photochemistry from **10** indicates the sensitive nature of excited-state deprotonation with respect to substituents. Further work will be needed to understand the factors that influence the operation of these substituent effects, which may be quite subtle.

## Experimental

### General

$^1\text{H}$  NMR spectra were obtained on Bruker AC300 or JEOL FX90Q instruments in  $\text{CDCl}_3$  unless otherwise specified. Low-resolution mass spectra were obtained on a Finnigan 3300 (CI) and HR-MS were obtained on a Kratos Concept H (EI) instrument. UV-vis spectra were recorded on a Varian Cary 5 instrument. Acetonitrile (HPLC grade) and distilled water were used for product studies and LFP experiments. Reagent grade  $\text{CH}_2\text{Cl}_2$  was redistilled before use for work-up protocols. The following buffers (0.01 M) were used for some product studies and LFP static and flow cell experiments: potassium phosphate – phosphoric acid (pH 3), acetate – acetic acid (pH 4 and 5), potassium phosphate (pH 6–8), sodium carbonate – sodium bicarbonate (pH 9–11). Aqueous  $\text{H}_2\text{SO}_4$  and NaOH were used for solutions at other pH values.

### Materials

*p*-Nitrobenzaldehyde (**15**) and *p*-nitrobenzophenone (**21**) (Aldrich) were recrystallized (ethanol– $\text{H}_2\text{O}$ ) prior to use. Sodium hexachloroiridate(IV) hexahydrate 99.9+% (Strem) was used without further purification. Product **18** was prepared by substitution of *p*-nitrobenzyl bromide with sodium acetate. An authentic sample of product **22** was prepared by reduction of **21** with paraformaldehyde–KOH, as described elsewhere (27).

### O-Acetyl *p*-nitromandelic acid (7)

A stirred suspension of 4-nitrophenylacetic acid (15.3 g, 84.5 mmol) in thionyl chloride (6.66 mL, 91.3 mmol) was refluxed for 1 h. The solution was allowed to cool and bromine (14.9 g, 93 mmol) was added in one portion. The mixture was heated at  $70^\circ\text{C}$  for 5.5 h and stirred overnight at room temperature. Ice water was added and the mixture was extracted with  $\text{Et}_2\text{O}$ . The organic phase was washed with brine, dried and evaporated to a brown oil (22 g) that was dissolved in a mixture of THF (230 mL) and water (100 mL) and stirred for 6 h at room temperature. The solution was concentrated under reduced pressure to remove most of the THF and water (50 mL) was added. The mixture was extracted with  $\text{Et}_2\text{O}$  and the ethereal extract was washed with brine, dried and evaporated to give a solid (18.5 g) that contained the starting nitrophenylacetic acid and the product **11** (typical ratio  $\sim 1:4$ ). After two crystallizations from

benzene–hexanes, the contamination by starting material was reduced to 8% and this material (11.7 g) was used without further processing. Within the mixture, **11** had  $^1\text{H NMR}$   $\delta$ : 8.22 (d,  $J = 8.8$  Hz, 2H, Ar-H), 7.73 (d,  $J = 8.8$  Hz, 2H, Ar-H), 5.40 (s, 1H, CHBr).

A mixture of the impure bromo compound **11** (11.49 g, 41.65 mmol) and mercury(II) acetate (28.2 g, 88.4 mmol) in glacial acetic acid (88 mL) was refluxed for 0.5 h. The solution was cooled, diluted with water, and extracted with  $\text{Et}_2\text{O}$ . The ether phase was washed with water and brine, dried and evaporated under reduced pressure. The residue was crystallized from water to give the acetate **7** (7.5 g, 37%), mp 153 to 154°C (lit. mp (28) 157–159°C).  $^1\text{H NMR}$   $\delta$ : 8.25 (d,  $J = 8.8$  Hz, 2H, Ar-H), 7.69 (d,  $J = 8.8$  Hz, 2H, Ar-H), 6.04 (s, 1H, CHOAc), 2.23 (s, 3H, Me).

#### **p-Nitromandelic acid (6)**

*tert*-Butyl 2,2,2-trichloroacetimidate (4.0 g, 18.3 mmol) in  $\text{CH}_2\text{Cl}_2$  (32 mL) was added in one portion to a solution of **7** (2.73 g, 11.4 mmol) in  $\text{CH}_2\text{Cl}_2$  (69 mL) and the solution was stirred overnight at room temperature. The mixture was diluted with  $\text{CH}_2\text{Cl}_2$ , washed with saturated  $\text{NaHCO}_3$ , water, and brine, dried and evaporated. The residue was dissolved in  $\text{Et}_2\text{O}$  (~10 mL) and most of the trichloroacetamide was precipitated by the addition of hexanes (~40 mL). The filtrate was evaporated and purified by flash chromatography (EtOAc–hexanes, 3:17) to give *tert*-butyl acetoxy-(4-nitrophenyl)acetate (**12**) as a yellow solid, (2.56 g, 76%). A sample crystallized from hexanes had mp 80 to 81°C (lit. mp (28) 82°C).  $^1\text{H NMR}$   $\delta$ : 8.24 (d,  $J = 8.8$  Hz, 2H, Ar-H), 7.66 (d,  $J = 8.8$  Hz, 2H, Ar-H), 5.91 (s, 1H, CHOAc), 2.23 (s, 3H, Me), 1.41 (s, 9H,  $\text{CMe}_3$ ).

A solution of **12** (2.53 g, 8.6 mmol) in methanol (25 mL) was treated with cesium carbonate (0.14 g, 0.43 mmol) in methanol (5 mL) and stirred for 0.5 h at room temperature. The solution was diluted with EtOAc, washed with satd.  $\text{NaHCO}_3$  and brine, dried and evaporated under reduced pressure. The residue was purified by flash chromatography (EtOAc–hexanes, 3:17) to give *tert*-butyl hydroxy-(4-nitrophenyl)acetate (**13**) (1.51 g, 70%), mp 91.5–93°C (hexanes).  $^1\text{H NMR}$   $\delta$ : 8.21 (d,  $J = 8.8$  Hz, 2H, Ar-H), 7.63 (d,  $J = 8.8$  Hz, 2H, Ar-H), 5.16 (d,  $J_{\text{H,OH}} = 4.5$  Hz, 1H, CHOH), 3.72 (d,  $J_{\text{H,OH}} = 4.5$  Hz, 1H, OH), 1.42 (s, 9H,  $\text{CMe}_3$ ). Anal. calcd. for  $\text{C}_{12}\text{H}_{15}\text{NO}_5$ : C 56.91, H 5.97, N 5.53; found: C 56.75, H 5.97, N 5.38.

The *tert*-butyl ester **13** (1.8 g, 7.1 mmol) was stirred with trifluoroacetic acid (36 mL) for 1 h at room temperature, then evaporated under reduced pressure to a brown gum which solidified on trituration with  $\text{Et}_2\text{O}$ . The solid was crystallized twice from toluene to give **6** as yellow needles (0.7 g, 48%), mp 128.5–130°C (lit. mp (29) 126 to 127°C).  $^1\text{H NMR}$  ( $\text{CD}_3\text{OD}$ )  $\delta$ : 8.25 (d,  $J = 8.8$  Hz, 2H, Ar-H), 7.69 (d,  $J = 8.8$  Hz, 2H, Ar-H), 5.26 (s, 1H, CHOH).

#### **p-Nitrobenzhydrol (9)**

Reduction of *p*-nitrobenzophenone (**21**) (Aldrich) with  $\text{NaBH}_4$  gave a white solid, which upon recrystallization from ethanol– $\text{H}_2\text{O}$  gave white crystals of *p*-nitrobenzhydrol (**9**), mp 69 to 70°C. IR (KBr disc,  $\text{cm}^{-1}$ ): 1190 (m), 1340 (s), 1450 (m), 1510 (s), 1600 (m), 3300–3500 (s).  $^1\text{H NMR}$  (300 MHz)  $\delta$ : 2.37 (s, 1H, exchanges with  $\text{D}_2\text{O}$ , OH), 5.90 (s, 1H, methine), 7.33 (m, 5H, arom.), 7.56 (d,  $J = 8.8$  Hz,

2H, arom.), 8.17 (d,  $J = 8.8$  Hz, 2H). HR-MS (EI) calcd. for  $\text{C}_{13}\text{H}_{11}\text{NO}_3$ : 229.0739; found: 229.0739.

#### **p-Nitrobenzhydrol methyl ether (10)**

A solution of **9** (300 mg) in methanol (50 mL) (in the presence of 10% concd  $\text{H}_2\text{SO}_4$ ) was refluxed for 24 h. Addition of ether and washing with  $\text{H}_2\text{O}$  resulted in extraction of a light yellow oil which by  $^1\text{H NMR}$  was found to contain 5% **9** and 95% **10**. Preparative TLC ( $\text{CH}_2\text{Cl}_2$  and silica gel) allowed isolation of a colourless oil ( $R_f$  0.9) *p*-nitrobenzhydrol methyl ether (**10**). IR (neat,  $\text{cm}^{-1}$ ): 1090 (s), 1190 (m), 1350 (s), 1450 (m), 1520 (s), 1600 (m).  $^1\text{H NMR}$  (300 MHz)  $\delta$ : 3.38 (s, 3H, methyl), 5.29 (s, 1H, methine), 7.30 (m, 5H, arom.), 7.51 (d,  $J = 8.8$  Hz, 2H, arom.), 8.16 (d,  $J = 8.8$  Hz, 2H, arom.). HR-MS (EI) calcd. for  $\text{C}_{14}\text{H}_{13}\text{NO}_3$ : 243.0896; found: 243.0893.

#### **$\alpha,\alpha'$ -Bisacetoxy-*p,p'*-dinitrobenzyl (19)**

Esterification of the corresponding diol (0.5 g), which was available from a previous study (21), in refluxing (10 h) glacial acetic acid (in the presence of 10% concd  $\text{H}_2\text{SO}_4$ ) gave 89% yield of an approximate 1:1 mixture of *cis*- and *trans*- $\alpha,\alpha'$ -bisacetoxy-*p,p'*-dinitrobenzyl (**19**). Recrystallization from ethyl acetate – hexanes enriched one of the diastereomers, thus allowing distinction between the  $^1\text{H NMR}$  signals of the two diastereomers. IR (mixture of diastereomers, KBr disc,  $\text{cm}^{-1}$ ): 1220 (s), 1350 (s), 1460 (w), 1530 (s), 1610 (m), 1750 (s).  $^1\text{H NMR}$  (300 MHz) diastereomer A (40%)  $\delta$ : 2.07 (s, 6H,  $\text{COCH}_3$ ), 6.14 (s, 2H, methine), 7.34 (d,  $J = 8.8$  Hz, 4H, arom.), 8.16 (d,  $J = 8.8$  Hz, 4H, arom.).  $^1\text{H NMR}$  (300 MHz) diastereomer B (60%)  $\delta$ : 2.10 (s, 6H,  $\text{COCH}_3$ ), 6.11 (s, 2H, methine), 7.33 (d,  $J = 8.8$  Hz, 4H, arom.), 8.13 (d,  $J = 8.8$  Hz, 4H, arom.). MS (mixture of diastereomers, + LSI-MS) 389 *m/e* ( $\text{M}^+ + 1$ ).

#### **Product studies**

UV–vis photolyses were carried out for 3 mL of the appropriate solution in Suprasil quartz cuvettes. Immediately before photolysis, each sample was Ar or  $\text{O}_2$  purged for 5 min, then quickly sealed with a Teflon stopper. During the photolysis the cuvette sat on top of an inverted 1 L beaker inside the Rayonet reactor (300 nm, 4–16 lamps) and was cooled with an internal fan. Irradiations did not exceed 10 min (total photolysis time); no heating of the samples was observed.

Preparative photolyses were carried out with the substrate (20–100 mg) dissolved in the appropriate solvent (100 mL) in a quartz tube. The solution was irradiated at 300 nm (Rayonet reactor, 4–16 lamps) with continuous cooling (by a cold finger) and purging by a stream of Ar for approximately 15 min before and continuously during irradiation (via a long stainless steel needle). Photolysis times ranged from 1 min to 20 h, depending on the conversion desired, the efficiency of the reaction, and the amount of substrate used. After photolysis, aqueous samples were acidified to pH 1 to 2 and extracted with  $\text{CH}_2\text{Cl}_2$ . Typical experiments are described below.

#### **Photolysis of *p*-nitromandelic acid (6) in 1:1 $\text{H}_2\text{O}$ – $\text{CH}_3\text{CN}$ (pH 7)**

A solution of **6** (20 mg) in 1:1  $\text{H}_2\text{O}$ – $\text{CH}_3\text{CN}$  (100 mL, pH adjusted to 7 with NaOH, Ar purged) was photolyzed for

2 min (300 nm, 16 lamps). After work-up,  $^1\text{H}$  NMR of the photolysate allowed observation of two aldehyde products (60% **15**, 40% **16**) and **6** (36% total conversion). Preparative TLC ( $\text{CH}_2\text{Cl}_2$  and silica gel) allowed isolation of the two products, one of which was identified as **15** ( $R_f$  0.5) by comparison with an authentic sample; the other ( $R_f$  0.3) identified as *p,p'*-azoxybisbenzaldehyde (**16**), mp 192°C. IR (KBr disc,  $\text{cm}^{-1}$ ): 1200 (m), 1320 (m), 1460 (m), 1600 (m), 1700 (s).  $^1\text{H}$  NMR  $\delta$ : 8.01 (d,  $J = 8.1$  Hz, 2H, arom.), 8.05 (d,  $J = 8.1$  Hz, 2H, arom.), 8.26 (d,  $J = 8.1$  Hz, 2H, arom.), 8.49 (d,  $J = 8.1$  Hz, 2H, arom.), 10.05 (s, 1 H, CHO), 10.14 (s, 1 H, CHO). HR-MS (EI) calcd. for  $\text{C}_{14}\text{H}_{10}\text{N}_2\text{O}_3$ : 254.0692; found: 254.0689.

#### Photolysis of *p*-nitromandelic acid (**6**) in 1:1 $\text{H}_2\text{O}$ - $\text{CH}_3\text{CN}$ (pH 3)

A solution of **6** (20 mg) in 1:1  $\text{H}_2\text{O}$ - $\text{CH}_3\text{CN}$  (100 mL, pH 3, 0.01 M phosphate buffer, Ar purged) was photolyzed for 5 min (300 nm, 16 lamps). Following work-up,  $^1\text{H}$  NMR allowed observation of the aldehyde peaks of **15** and **16**, as well as an aldehyde signal which had not been present in the pH 7 product studies. Based on integration the relative yields of these products were 50% (**15**), 22% (**16**) and 28% of the new aldehyde product, and the total conversion from substrate was 61%. This procedure was repeated until approximately 90 mg of photolysate had been collected. An initial attempt to separate the new product via preparative TLC ( $\text{CH}_2\text{Cl}_2$  and silica gel) resulted in recovery of **15** and the new product in one band ( $R_f$  0.6). A second attempt (1:9 ethyl acetate:hexanes and silica gel) succeeded in separating **15** ( $R_f$  0.2) from the new light yellow product ( $R_f$  0.3), identified as *p*-nitrosobenzaldehyde (**17**) (based on identical  $^1\text{H}$  NMR with that reported in the literature (30)). IR (KBr disc,  $\text{cm}^{-1}$ ): 1200 (m), 1260 (s), 1390 (m), 1460 (w), 1595 (m), 1690 (s).  $^1\text{H}$  NMR  $\delta$ : 8.03 (d,  $J = 8.8$  Hz, 2H, arom.), 8.17 (d,  $J = 8.1$  Hz, 2H, arom.), 10.20 (s, 1H, CHO). HR-MS (EI) calcd. for  $\text{C}_7\text{H}_5\text{NO}_2$ : 135.0321; found: 135.0323.

#### Photolysis of *O*-acetyl *p*-nitromandelic acid (**7**) in 1:1 $\text{H}_2\text{O}$ - $\text{CH}_3\text{CN}$ (pH 7)

A solution of **7** (20 mg) in 1:1  $\text{H}_2\text{O}$ - $\text{CH}_3\text{CN}$  (100 mL, pH adjusted to 7, Ar purged) was photolyzed for 20 min (300 nm, 4 lamps). Following work-up,  $^1\text{H}$  NMR of the photolysate revealed 23% conversion to **18** and **19** (47 and 53%, respectively), each of which were identified by addition of an authentic sample (vide supra) which enhanced the  $^1\text{H}$  NMR signals.

#### Photolysis of *p*-nitrophenylethylene glycol (**8**) in 1:1 $\text{H}_2\text{O}$ - $\text{CH}_3\text{CN}$ (pH 13)

A solution of **8** (100 mg) in 1:1  $\text{H}_2\text{O}$ - $\text{CH}_3\text{CN}$  (100 mL, pH 13, Ar purged) was photolyzed for 30 min (300 nm, 16 lamps). Following work-up  $^1\text{H}$  NMR of the photolysate revealed 69% conversion to **15** and **16** (60 and 40%, respectively), identified as above (vide supra).

#### Photolysis of *p*-nitrobenzhydrol (**9**) in 1:1 $\text{H}_2\text{O}$ - $\text{CH}_3\text{CN}$ (pH 13)

A solution of **9** (20 mg) in 1:1  $\text{H}_2\text{O}$ - $\text{CH}_3\text{CN}$  (100 mL, pH 13, Ar purged) was photolyzed for 60 min (300 nm, 16 lamps). After photolysis the solution turned a deep red color

that did not dissipate for up to several hours. Upon acidification to pH 2 with aq HCl, the color turned to yellow (between pH 10 and 11), with formation of a yellow precipitate. Extraction of the whole mixture with  $\text{CH}_2\text{Cl}_2$  gave a  $^1\text{H}$  NMR that showed ~15% conversion of **9** to **21** and **22** (70 and 30%, respectively), and a third, unidentified product. In a separate experiment, the precipitate formed during acidification was isolated by suction filtration and found to contain **22** and the unidentified product (in a ~1:1 mixture), while the filtrate contained **9** and **21**. Preparative TLC ( $\text{CH}_2\text{Cl}_2$  and silica gel) failed to separate **22** from the unidentified product. Based on analysis of the  $^1\text{H}$  NMR pattern of the unidentified product (as a mixture with **22**), we have tentatively identified it as a secondary photoproduct of **22**, i.e., a hydroxyazobenzene derived from **22**, consistent with the known photo-Wallach rearrangement of aromatic azoxy compounds (31).

#### Quantum yields

The quantum yield of **6** was measured by preparative photolysis and  $^1\text{H}$  NMR using **3** as secondary actinometer ( $\Phi = 0.6$ ) (12). Photolysis of **3** (20 mg, pH 7, 100 mL 100% 0.01 M phosphate buffer, 300 nm, 4 lamps, 2 min, Ar purged) followed by assessment of the conversion to product (10–15%) allowed calculation of the number of photons emitted by the apparatus. In a following photolysis of **6** (100% pH 6 0.01 M phosphate buffer) using identical conditions, assessment of conversion (5–10%) allowed calculation of the quantum yield for the reaction. These photolyses were repeated four times, and the average quantum yield was calculated.

#### Laser flash photolysis (LFP)

LFP data was acquired using either a Nd:YAG laser (Spectra-Physics Quanta-Ray GCR-11,  $\lambda_{\text{ex}}$  266 nm; this laser was used for most LFP experiments) or a Lumonics excimer laser (EX-510,  $\lambda_{\text{ex}}$  308 nm; this laser was used for experiments using  $\text{IrCl}_6^{2-}$ ) with pulse widths ~20 ns and power attenuated to ~20 mJ/pulse. Signals were digitized with a Tektronix TDS 520 recorder. Solutions with OD = 0.3 at  $\lambda_{\text{ex}}$  were used to ensure even penetration of the laser light. Quartz flow cells were used for all studies except for the measurement of  $\Delta\text{OD}_{\text{init}}$  at various pH values (Figs. 10 and 12), where quartz static cells were used. Samples in flow cells were continuously purged with a stream of  $\text{N}_2$  or  $\text{O}_2$  for 15 min before and during the experiment. Samples in static cells were purged with  $\text{N}_2$  or  $\text{O}_2$  for 5 min and subsequently sealed prior to the experiment. The contents of static cells were mixed between each laser shot to avoid depletion of the solution in the irradiated volume.

#### Acknowledgments

We thank the Natural Sciences and Engineering Research Council of Canada (NSERC) for continued support of this research, and Mr. Xigen Xu for the initial studies on compound **8**.

## References

1. D.J. Cram. *Fundamentals of carbanion chemistry*. Academic Press Inc., New York. 1965. p. 289.
2. P.M. Mayer and L. Radom. *J. Phys. Chem. A*, **102**, 4918 (1998).
3. K.M. Downard, J.C. Sheldon, J.H. Bowie, D.E. Lewis, and R.N. Hayes. *J. Am. Chem. Soc.* **111**, 8112 (1989).
4. P. Wan and K. Yates. *Can. J. Chem.* **64**, 2076 (1986).
5. P. Wan and X. Xu. *Tetrahedron Lett.* **31**, 2809 (1990).
6. J. Morrison, H. Osthoff, and P. Wan. *Photochem. Photobiol. Sci.* **1**, 384 (2002).
7. M. St. Maurice and S.L. Bearne. *Biochemistry*, **39**, 13324 (2000).
8. M. Garcia-Viloca, A. Gonzalez-Lafont, and J.M. Lluch. *J. Am. Chem. Soc.* **123**, 709 (2001).
9. P.K. Das. *Chem. Rev.* **93**, 119 (1993).
10. T.-I. Ho and Y.L. Chow. *In The chemistry of amino, nitroso and related groups*. Vol. 1. *Edited by S. Patai*. John Wiley and Sons, Toronto. 1996. p. 747.
11. D. Döpp. *In CRC handbook of organic photochemistry and photobiology*. *Edited by W.M. Horspool and P.-S. Song*. CRC Press, Boca Raton. 1995. Chap. 81. p. 1019.
12. J.D. Margerum and C.T. Petrusis. *J. Am. Chem. Soc.* **91**, 2467 (1969).
13. P. Wan and S. Muralidharan. *J. Am. Chem. Soc.* **110**, 4336 (1988).
14. G.A. Russell, A.J. Moye, E.G. Janzen, S. Mak, and E.R. Talaty. *J. Org. Chem.* **32**, 137 (1967).
15. G.A. Russell and E.G. Janzen. *J. Am. Chem. Soc.* **89**, 300 (1967).
16. E. Buncl and B.C. Menon. *J. Am. Chem. Soc.* **102**, 3499 (1980).
17. B.B. Craig, R.G. Weiss, and S.J. Atherton. *J. Phys. Chem.* **91**, 5906 (1987).
18. B.B. Craig and S.J. Atherton. *J. Chem. Soc., Perkin Trans. 2*, 1929 (1988).
19. A. McKenzie and P.A. Stewart. *J. Chem. Soc.* 104 (1935).
20. G. Carrara, F. Fava, C. Martinuzzi, and A. Vecchi. *Gazz. Chim. Ital.* **82**, 674, (1952).
21. S. Muralidharan and P. Wan. *J. Photochem. Photobiol. A*, **57**, 191 (1991).
22. T. Shida. *Electronic absorption spectra of radical ions*. Elsevier, New York. 1988.
23. S. Steenken and P. Neta. *J. Am. Chem. Soc.* **104**, 1244 (1982).
24. J. Halpern, R.J. Legare, and R. Lumry. *J. Am. Chem. Soc.* **85**, 680 (1963).
25. J.Y. Chen, H.C. Gardner, and J.K. Kochi. *J. Am. Chem. Soc.* **98**, 6150 (1976).
26. M. Schwörer and J. Wirz. *Helv. Chim. Acta*, **84**, 1441 (2001).
27. R.B. Davis and J.D. Benigni. *J. Org. Chem.* **27**, 1605 (1962).
28. K. Schank. *Chem. Ber.* **103**, 3093 (1970).
29. G. Heller. *Chem. Ber.* **46**, 280 (1913).
30. X. Creary, P.S. Engel, N. Kavaluskas, L. Pan, and A. Wolf. *J. Org. Chem.* **64**, 5634 (1999).
31. N.J. Bunce, J.P. Schoch, and M.C. Zerner. *J. Am. Chem. Soc.* **99**, 7986 (1977).